

# SCIENTIFIC REPORTS

OPEN

## Remarkably High Mobility Thin-Film Transistor on Flexible Substrate by Novel Passivation Material

Cheng Wei Shih &amp; Albert Chin

High mobility thin-film transistor (TFT) is crucial for future high resolution and fast response flexible display. Remarkably high performance TFT, made at room temperature on flexible substrate, is achieved with record high field-effect mobility ( $\mu_{FE}$ ) of  $345 \text{ cm}^2/\text{Vs}$ , small sub-threshold slope (SS) of  $103 \text{ mV}/\text{dec}$ , high on-current/off-current ( $I_{ON}/I_{OFF}$ ) of  $7 \times 10^6$ , and a low drain-voltage ( $V_D$ ) of  $2 \text{ V}$  for low power operation. The achieved mobility is the best reported data among flexible electronic devices, which is reached by novel HfLaO passivation material on nano-crystalline zinc-oxide (ZnO) TFT to improve both  $I_{ON}$  and  $I_{OFF}$ . From X-ray photoelectron spectroscopy (XPS) analysis, the non-passivated device has high OH-bonding intensity in nano-crystalline ZnO, which damage the crystallinity, create charged scattering centers, and form potential barriers to degrade mobility.

The flexible electronics is the key technology for bendable light weight display<sup>1-7</sup>. Similar to traditional rigid displays, the higher mobility TFT<sup>1-24</sup> is demanded for next generation higher density, faster speed, and lower power flexible display<sup>6</sup>. The amorphous InZnGaO (IGZO) TFT<sup>5-10</sup> is a potential candidate for flexible electronics due to the low off-current ( $I_{OFF}$ ) from its large energy bandgap and high mobility of overlapped s-orbitals. However, the major issue for IGZO TFT is the rare Indium quantity in Earth's crust and its high price. Alternatively, crystallized ZnO TFT is another candidate due to its better crystallinity than amorphous structure, similar with the much higher mobility of poly-Si than amorphous-Si TFTs. However, no high mobility poly-ZnO TFT was reported to date. In this paper, we demonstrate a high performance nano-crystallized ZnO TFT on low-cost Polyethylene naphthalate (PEN) flexible substrate processed at room temperature. Remarkably high  $\mu_{FE}$  of  $345 \text{ cm}^2/\text{Vs}$  was achieved in nano-crystalline ZnO TFT on flexible substrate with a high dielectric constant (high- $\kappa$ ) gate oxide<sup>25-29</sup>. This  $\mu_{FE}$  value is even higher than IGZO and ZnON TFTs made on rigid glass<sup>22,23</sup> that is also the record highest value for devices on flexible substrate<sup>1-7</sup>. The high mobility is further supported by the low interface trap density from the small SS of only  $103 \text{ mV}/\text{dec}$ . Besides, high  $I_{ON}/I_{OFF}$  of  $7 \times 10^6$  and a low  $V_D$  of  $2 \text{ V}$  were measured to reach low switching power of  $C_G V_D^2 f / 2$ , where  $C_G$  and  $f$  are the gate capacitance and operation frequency, respectively. This remarkably high mobility TFT is achieved using novel HfLaO passivation on nano-crystalline ZnO. For comparison, the control non-passivated device has a  $\mu_{FE}$  of  $43 \text{ cm}^2/\text{Vs}$ . To understand such large mobility improvement, the X-ray photoelectron spectroscopy (XPS) was performed. The non-passivated ZnO showed a strong OH bonding signal. The formed HO-Zn-OH compound via moisture absorption will break the Zn-O bonding in ZnO crystal to form dangling bonds and charged scattering centers to lower the mobility strongly. In contrast to other passivation methods<sup>14-21</sup>, the LaO-based dielectric has important advantage of moisture absorption to lower the OH bonding formation as evident from the XPS data<sup>25-29</sup>. The remarkably high  $\mu_{FE}$  HfLaO/ZnO TFT suggests the excellent opportunity for both flexible and rigid display applications.

### Results

The fabricated devices on flexible PEN substrate is shown in the photo of Fig. 1. Figure S1(a,b) show the capacitance-voltage ( $C-V$ ) and current-voltage ( $J-V$ ) characteristics of Al/high- $\kappa$  metal-gate capacitor fabricated on the same flexible PEN substrate, respectively. A high capacitance density of  $0.35 \mu\text{F}/\text{cm}^2$  was measured that lead to an equivalent-oxide-thickness (EOT) of  $9.9 \text{ nm}$ . A still low leakage current of  $1.4 \times 10^{-5} \text{ A}/\text{cm}^2$  was measured at  $1.5 \text{ V}$ , even processed at room temperature. This is due to the merit of high- $\kappa$  dielectrics, especially the

Department of Electronics Engineering, National Chiao Tung University, Hsinchu, 300, Taiwan. Correspondence and requests for materials should be addressed to A.C. (email: [achin@faculty.nctu.edu.tw](mailto:achin@faculty.nctu.edu.tw))

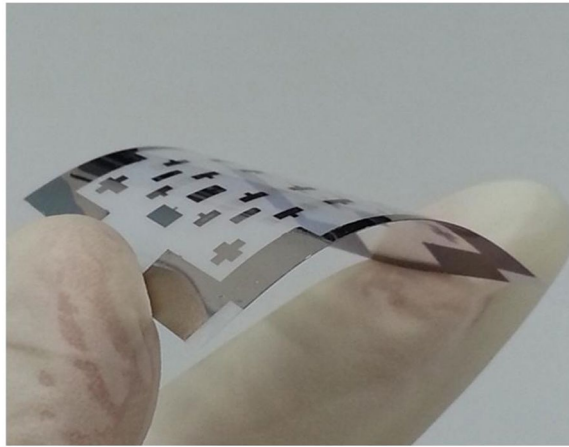


**Figure 1.** Device photo of fabricated TFTs on flexible PEN substrate.

higher  $\kappa$   $\text{TiO}_2$  dielectric. The  $\text{TiO}_2$  has higher  $\kappa$  value for low voltage operation. To improve the interface<sup>30</sup>, extra  $\text{SiO}_2$  dielectric was inserted between ZnO and  $\text{TiO}_2$ . To improve the leakage current via the low conduction band offset ( $\Delta E_C$ ) of  $\text{TiO}_2$ , stacked  $\text{TiO}_2/\text{HfO}_2$  were applied<sup>31</sup>.

Figure 2(a–c) show the transistor's drain-source current versus drain-source voltage ( $I_{DS}-V_{DS}$ ) and  $I_{DS}$  versus gate-source voltage ( $I_{DS}-V_{GS}$ ) characteristics of ZnO/high- $\kappa$ /metal-gate TFTs with and without HfLaO passivation. The ZnO TFTs without passivation show reasonable performance of  $I_{ON}/I_{OFF}$  of  $2 \times 10^5$ , SS of 112 mV/dec, and a  $V_T$  of 0.78 V. Here the gate leakage current is lower than  $I_{OFF}$  due to the thick stacked gate dielectric. The ZnO TFTs after HfLaO passivation shows more than one order of magnitude higher  $I_{ON}$  and 4 times lower  $I_{OFF}$ , with large  $I_{ON}/I_{OFF}$  of  $7 \times 10^6$ , small SS of 103 mV/dec, and a low  $V_T$  of 0.13 V. These good device integrities were achieved at a low  $V_D$  of 2 V that is crucial to lower the switching power by orders of magnitude than existing TFT devices. Besides, the steep SS can also turn on the transistor faster for a lower voltage and power operation.

The  $\mu_{FE}-V_{GS}$  characteristics is plotted in Fig. 3 from the measured  $I_{DS}-V_{GS}$  characteristics. For control non-passivated devices, an acceptable peak  $\mu_{FE}$  of 43  $\text{cm}^2/\text{Vs}$  is obtained for room-temperature-processed ZnO TFT. The TFT devices after HfLaO passivation has remarkably high  $\mu_{FE}$  of 345  $\text{cm}^2/\text{Vs}$ ; this is the highest value for TFT on flexible substrate<sup>1–7</sup> and is even higher than the reported IGZO and ZnON TFTs fabricated on rigid substrate<sup>22,23</sup>. The much improved  $\mu_{FE}$  for HfLaO-passivated device is owing to the higher  $I_{ON}$  and the lower  $I_{OFF}$ . It is important to notice that the  $\mu_{FE}$  decreases monotonically with decreasing gate length<sup>32,33</sup>.

$$\mu \approx \mu_0 \frac{L}{L + \mu_0 W C_{\alpha} R_{SD} (V_{GS} - V_{th})} \quad (1)$$

where  $R_{SD}$  is the source/drain series resistance,  $\mu_{FE}$  is the apparent field-effect mobility and  $\mu_0$  is the true field effect mobility. At long gate length, the  $\mu_{FE}$  is approaching to  $\mu_0$ ; thus, the long 48  $\mu\text{m}$  gate length device was used.

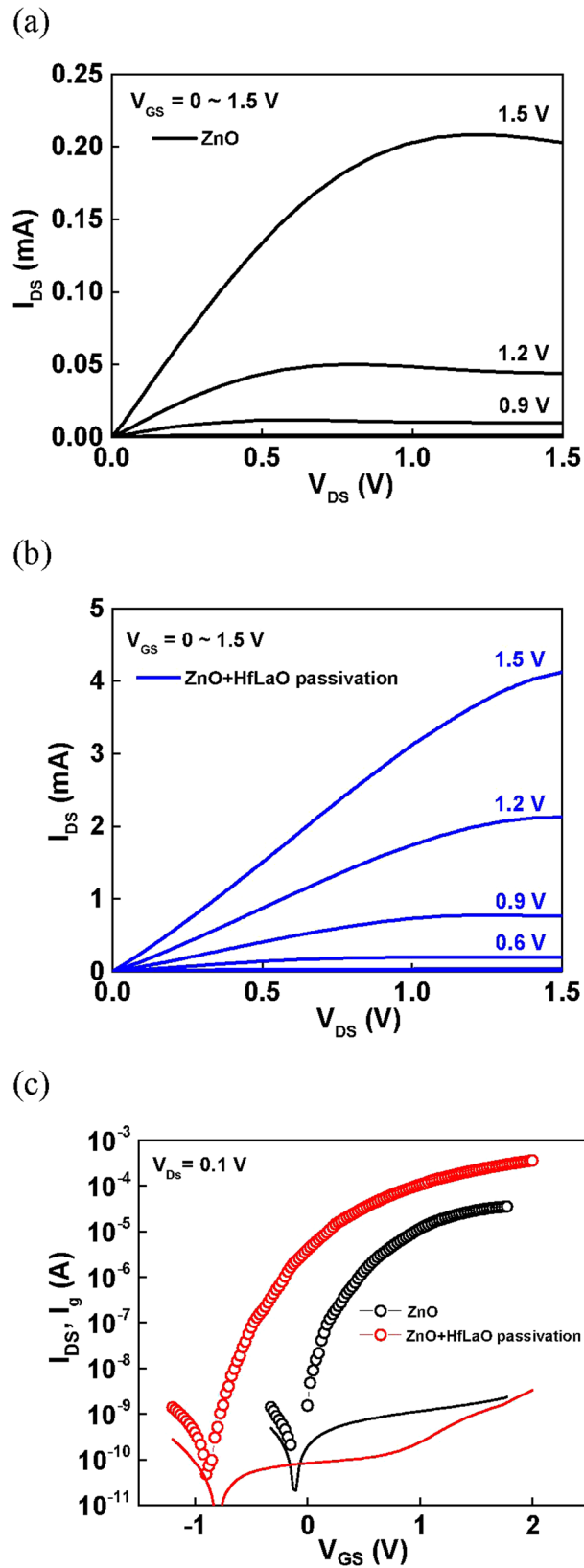
To understand the mechanism of such large mobility improvement, material and structure analysis were performed. Figure 4(a) shows the secondary ion mass spectrometry (SIMS) depth profile, where a ZnO channel,  $\text{HfO}_2$ ,  $\text{TiO}_2$ , and thin  $\text{SiO}_2$  gate dielectric stack were recognized. The device structure of Al contact, ZnO channel, high- $\kappa$  gate dielectric stack, and TaN metal-gate were also observable from the cross-sectional transmission electron microscopy (TEM) image shown in Fig. 4(b). The ZnO active layer forms columnar nano-crystalline structure with a size of  $\sim 10$ – $20$  nm. The formed crystalline structure is further evidenced from the X-ray diffraction (XRD) spectra shown in Fig. 4(c). Highly oriented phases of XRD peaks were measured, even though the ZnO was deposited by sputtering at room temperature. The full-width at half-maximum (FWHM) of XRD spectra are comparable with the data of ZnO published in literature<sup>34,35</sup>, while the IGZO has an amorphous structure<sup>36</sup>.

Figure 5(a,b) show the XPS spectra without and with HfLaO passivation, respectively. The atomic composition of nano-crystalline structure is identified to be  $\text{Zn}^{2+}-\text{O}^{2-}$ , as measured from the XPS spectra. It is important to notice that significant amount of OH bonding signal was also measured for non-passivated device. The OH bonding in nano-crystalline ZnO was originated from the moisture absorption of ambient air, even though dry process steps were used to fabricate the devices. Similar strong moisture absorption is well known in IGZO to cause degradation.

The chemical reaction of ZnO and  $\text{H}_2\text{O}$  is expressed as:



In addition to surface, the tiny  $\text{H}_2\text{O}$  molecule can also react with grain boundaries through the thin 20-nm ZnO. Here the grain boundaries are highly reactive due to their high defect density. Once the  $\text{Zn(OH)}_2$  was formed, it damaged the Zn-O bonded nano-crystal and created dangling bonds that further form charged states in the ZnO bandgap. The decreased XPS OH signal and related charged defects are also supported from the high positive charge density ( $\Delta Q_p$ ) of  $2 \times 10^{12} \text{ cm}^{-2}$ , which was obtained from the  $V_T$  shift ( $\Delta V_T$ ) between HfLaO-passivated and non-passivated ZnO devices shown in Fig. 3(b), from the  $\Delta Q_p = C_G \times \Delta V_T$ . Such positive



**Figure 2.**  $I_{DS}$ - $V_{DS}$  and characteristics of ZnO/high- $\kappa$ /TaN TFT on flexible PEN (a) without and (b) with HfLaO passivation. (c)  $I_{DS}$ - $V_{GS}$  characteristics of ZnO/high- $\kappa$ /TaN TFT on flexible PEN without and with HfLaO passivation.

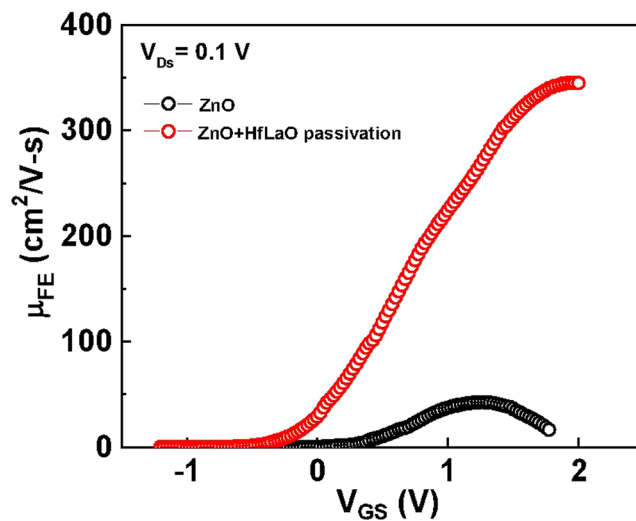


**Figure 3.** The  $\mu_{FE}$ - $V_{GS}$  characteristics of ZnO/high- $\kappa$ /TaN TFT on flexible PEN without and with HfLaO passivation.

Channel Materials	Channel layer thickness (nm)	Gate Insulator Materials	SS (V/decade)	$\mu_{FE}$ ( $\text{cm}^2/\text{V}\cdot\text{s}$ )	$I_{ON}/I_{OFF}$	Operating Voltage (V)
Flexible ZnO [1]	10	$\text{Al}_2\text{O}_3$	—	~32	$\sim 10^8$	8
Flexible $\text{MoS}_2$ [2]	~2.6	hBN	—	~40	$> 10^4$	80
Rigid ITO/IGZO [22]	5/70	$\text{SiO}_2$	~0.25	104	$> 10^7$	15
Rigid ZnON [23]	50	$\text{SiN}_x/\text{SiO}_2$	0.8	~115	$> 10^6$	20
Flexible This Work	20	$\text{HfO}_2/\text{TiO}_2/\text{SiO}_2$	0.103	345	$7 \times 10^6$	2

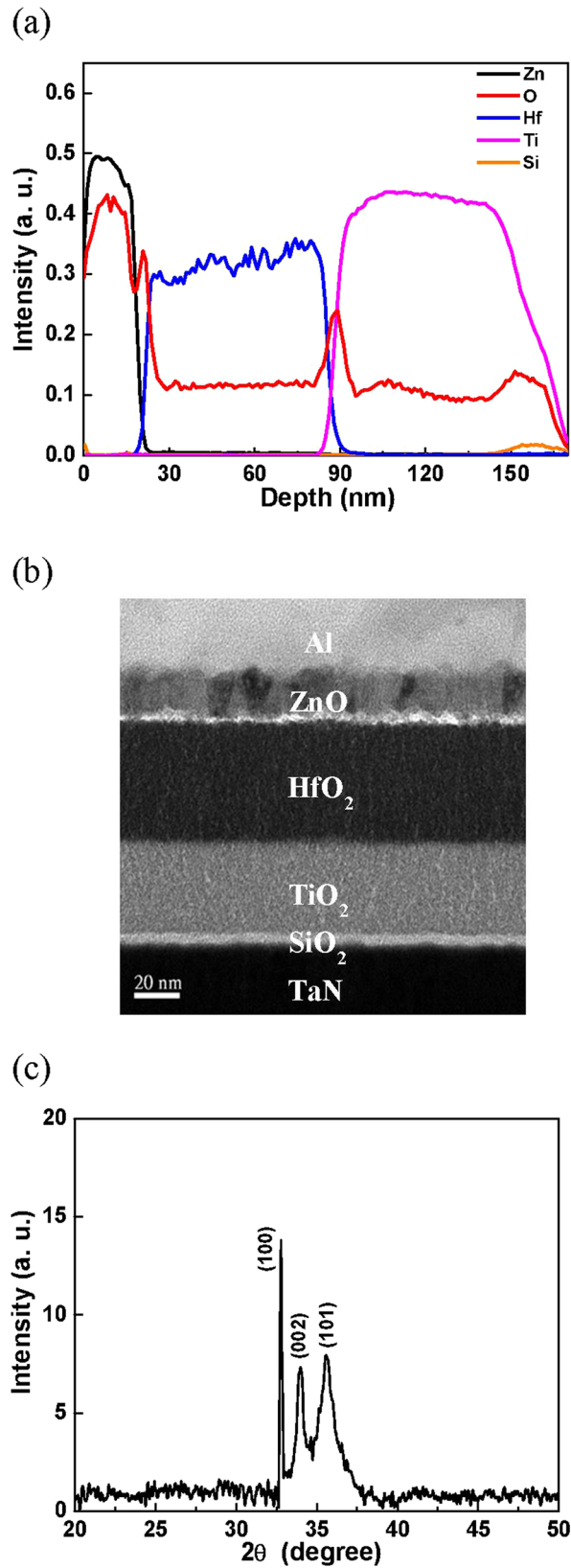
**Table 1.** Device performance comparison among flexible ZnO,  $\text{MoS}_2$ , and HfLaO-passivated ZnO TFTs (this work). The IGZO and ZnON TFTs on rigid glass substrate were also added for comparison.

charges and dangling bonds also found in the interim  $\text{SiO}_x$  region between  $\text{SiO}_2$  and Si body, the origin of positive fixed oxide charges in  $\text{SiO}_2/\text{Si}$  metal-oxide-semiconductor field-effect transistor (MOSFET) shown in text book. On the other hand, the OH bonding signal in XPS spectra of Fig. 5(b) is much lowered for HfLaO passivated ZnO device. It is well known the high- $\kappa$  gate dielectric will absorb the moisture<sup>25–29</sup>, especially the  $\text{La}_2\text{O}_3$ , which in turn reduce the  $\text{Zn}(\text{OH})_2$  formation.

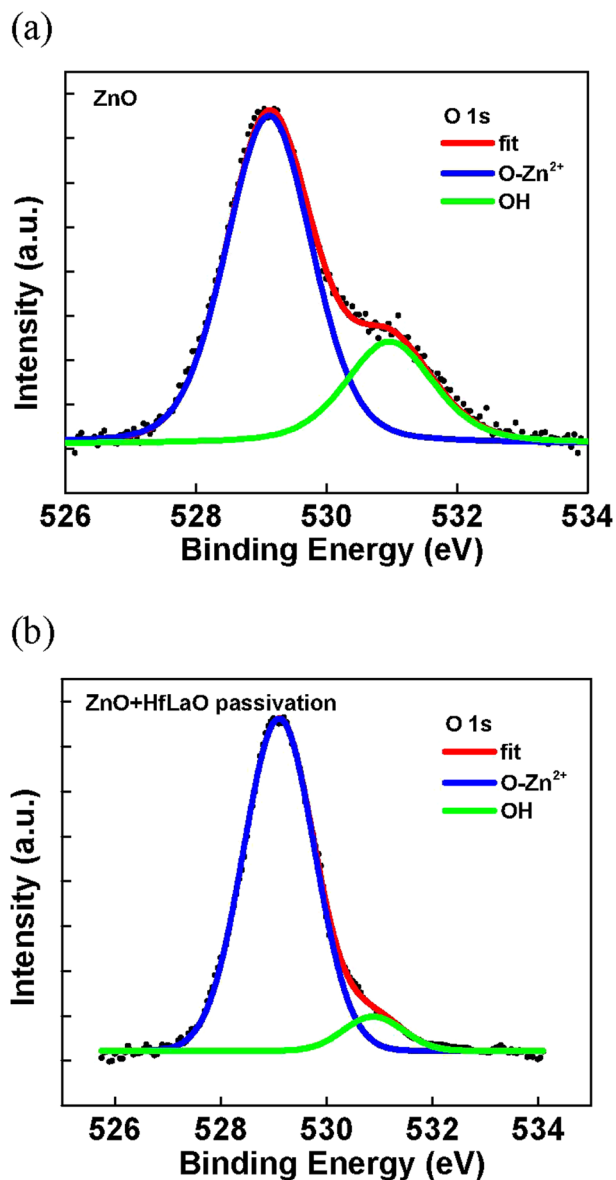
The high-density positive  $\Delta Q_p$  further causes Fermi-level closer to valence band, increases the ZnO depletion region, and lower the n-type ZnO conduction, as shown in the schematic diagrams of Fig. 6. The electron wave-function in a MOSFET typically distributes over 20 nm<sup>30</sup>, therefore the high-density  $\Delta Q_p$  will also increase electron scattering rate and decrease mobility. However, the passivation does not affect the gate EOT, because the EOT of a TFT only counts the dielectric next to the gate. Because proper passivation blocks the reaction between  $\text{H}_2\text{O}$  and ZnO, the OH bonding in HfLaO/ZnO is much reduced to lower  $\Delta Q_p$  and potential barriers at grain boundaries. This in succession leads to much higher mobility, because the ZnO has overlapped s-orbitals for conduction.

Table 1 compares the device performance of various materials on flexible and rigid substrates. The mobility of HfLaO-passivated ZnO TFT is higher than the IGZO and ZnON TFTs on rigid substrate<sup>22,23</sup> that is also the record highest value for TFTs on flexible substrate<sup>1–7</sup>. This is possible because the poly-crystalline material always has better material quality and higher mobility than amorphous structure, and the mobility improvement can be as large as ~100 times for poly-Si versus amorphous-Si TFTs. The very high mobility ZnO TFT with excellent SS, large  $I_{ON}/I_{OFF}$  and low  $V_D$  are vital for both DC and AC power saving. The simple process and low material cost of nano-crystalline ZnO device should have strong impact on next generation display, as long as OH bonding related charge traps and grain boundary potential barriers are improved by proper passivation. The achieved high mobility on amorphous material is also the enabling technology for high-speed 3D brain-mimicking chip<sup>24</sup>.

In conclusion, very high mobility, excellent SS, large  $I_{ON}/I_{OFF}$ , low  $V_D$ , and low power operation were achieved in ZnO TFT device that is crucial for display and 3D IC. The excellent device integrity is due to the novel passivation scheme with simple process.



**Figure 4.** (a) SIMS depth profile of ZnO on HfO<sub>2</sub>/TiO<sub>2</sub>/SiO<sub>2</sub> stacked gate dielectrics, (b) Cross-sectional TEM and (c) XRD spectra of ZnO/high-κ/TaN structure on flexible PEN substrate.



**Figure 5.** XPS spectra of ZnO/high- $\kappa$ /TaN structure on flexible PEN substrate (a) without and (b) with HfLaO passivation. Here the passivated HfLaO was removed for XPS measurement.

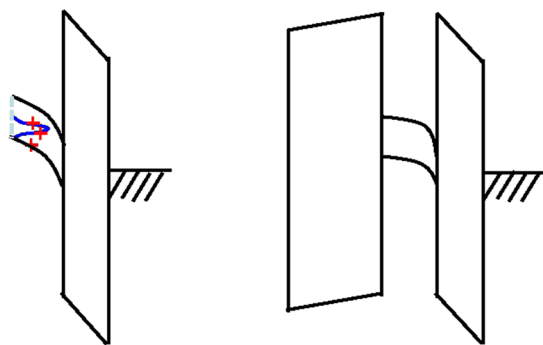


**Figure 6.** Schematic ZnO/high- $\kappa$ /TaN energy bands and nano-crystalline-ZnO band structures on flexible PEN without (left) and with (right) HfLaO-passivation.



## Methods

The bottom-gate ZnO/high- $\kappa$ /metal-gate TFTs were made on flexible polyethylene naphthalate (PEN) substrate. In addition to its low cost, the PEN substrate has good properties of a low linear thermal expansion coefficient, surface smoothness, and optical clarity. A 300-nm smoothing SiO<sub>2</sub> layer was first deposited on PEN substrate. Then the 60-nm TaN gate metal, tri-layer gate dielectrics of 50-nm HfO<sub>2</sub>, 40-nm TiO<sub>2</sub> and 4-nm-SiO<sub>2</sub>, and a 20-nm ZnO active layer were deposited by physical vapor deposition (PVD). Then the Al source/drain (S/D) electrodes was formed. Finally, the device was passivated by 20 nm thick HfLaO dielectric with opened S/D probing window. The TaN gate electrode was deposited by sputtering at a power of 800 W, Ar/N<sub>2</sub> of 100/10 sccm, and a pressure of  $3 \times 10^{-3}$  torr. The gate dielectric stacks were deposited by electron-gun evaporation at 5 KV, and the deposition rates were 0.24/0.2/0.1 Å/sec, respectively. The ZnO channel were deposited by sputtering at a power of 100 W, Ar/O<sub>2</sub> of 20/5 sccm, and 1 Å/sec deposition rate. The Al source-drain was deposited by thermal evaporation deposition. The HfLaO was deposited by electron-gun evaporation at a deposition rate of 0.15 Å/sec. Before deposition, the chambers were pumped down to  $3 \times 10^{-6}$  torr. The low deposition rate is important to reach good quality. No post-deposition annealing was used that is the merit of this work. The gate size of fabricated TFT is 48- $\mu$ m  $\times$  505- $\mu$ m. To investigate the large mobility improvement, X-ray diffraction (XRD), secondary ion mass spectrometry (SIMS), cross-sectional transmission electron microscopy (TEM), and X-ray photoelectron spectroscopy (XPS) were used to analyze the material property. Very low etching rate of 0.2 Å/sec was used in the XPS measurement due to the thin 20 nm HfLaO passivation layer.

## References

- Li, H. U. *et al.* ZnO thin film transistors for more than just displays. *IEDM Tech. Dig.* 523 (2015).
- Petroni, N., Cui, X., Hone, J., Chari, T. & Shepard, K. Flexible 2D FETs using hBN dielectrics. *IEDM Tech. Dig.* 534 (2015).
- Kao, H. L. *et al.* Strain-induced very low noise RF MOSFETs on flexible plastic substrate. *Symp. on VLSI Tech. Dig.* 160 (2005).
- Lin, Y. Y. *et al.* Stable and high-performance flexible ZnO thin-film transistors by atomic layer deposition. *ACS Appl. Mater. Interfaces* 7, 22610 (2015).
- Nomura, K. *et al.* Room-temperature fabrication of transparent flexible thin-film transistors using amorphous oxide semiconductors. *Nature* 432, 488, doi:10.1038/nature03090 (2004).
- Kamiya, T., Nomura, K. & Hosono, H. Present status of amorphous In–Ga–Zn–O thin-film-transistors. *Sci. Technol. Adv. Mater.* 11, 044305, doi:10.1088/1468-6996/11/4/044305 (2010).
- Su, N. C. *et al.* Low-voltage-driven flexible InGaZnO thin-film transistor with small subthreshold swing. *IEEE Electron Device Lett.* 31, 680, doi:10.1109/LED.2010.2047232 (2010).
- Zan, H. W., Yeh, C. C., Meng, H. F., Tsai, C. C. & Chen, L. H. Achieving high field-effect mobility in amorphous indium-gallium-zinc oxide by capping a strong reduction layer. *Adv. Mater.* 24, 3509, doi:10.1002/adma.201200683 (2012).
- Iwasaki, T. *et al.* Combinatorial approach to thin-film transistors using multicomponent semiconductor channels: An application to amorphous oxide semiconductors in In–Ga–Zn–O system. *Appl. Phys. Lett.* 90, 242114, doi:10.1063/1.2749177 (2007).
- Bak, J. Y. *et al.* Origin of degradation phenomenon under drain bias stress for oxide thin film transistors using IGZO and IGO channel layers. *Scientific Reports* 5, 7884, doi:10.1038/srep07884 (2015).
- Yang, C. *et al.* Solution-processed flexible ZnO transparent thin-film transistors with a polymer gate dielectric fabricated by microwave heating. *Nanotechnology* 20, 465201, doi:10.1088/0957-4484/20/46/465201 (2009).
- Park, J. S. *et al.* Flexible full color organic light-emitting diode display on polyimide plastic substrate driven by amorphous indium gallium zinc oxide thin-film transistors. *Appl. Phys. Lett.* 95, 013503, doi:10.1063/1.3159832 (2009).
- Lim, W. *et al.* Low-temperature-fabricated InGaZnO<sub>4</sub> thin film transistors on polyimide clean-room tape. *Appl. Phys. Lett.* 93, 252103, doi:10.1063/1.3054167 (2008).
- Jeong, J. K., Yang, H. W., Jeong, J. H., Mo, Y. G. & Kim, H. D. Origin of threshold voltage instability in indium-gallium-zinc oxide thin film transistors. *Appl. Phys. Lett.* 93, 123508, doi:10.1063/1.2990657 (2008).
- Park, J. *et al.* The influence of SiO<sub>x</sub> and SiN<sub>x</sub> passivation on the negative bias stability of Hf–In–Zn–O thin film transistors under illumination. *Appl. Phys. Lett.* 96, 262109, doi:10.1063/1.3435482 (2010).
- Yang, S. *et al.* Improvement in the photon-induced bias stability of Al–Sn–Zn–In–O thin film transistors by adopting AlO<sub>x</sub> passivation layer. *Appl. Phys. Lett.* 96, 213511, doi:10.1063/1.3432445 (2010).
- Cho, D. *et al.* Transparent Al–Zn–Sn–O thin film transistors prepared at low temperature. *Appl. Phys. Lett.* 93, 142111, doi:10.1063/1.2998612 (2008).
- Lee, K. *et al.* ZnO-based low voltage inverter with low-k/high-k double polymer dielectric layer. *Appl. Phys. Lett.* 93, 193514, doi:10.1063/1.3028093 (2008).
- Liu, S. E. *et al.* Influence of passivation layers on characteristics of a-InGaZnO thin-film transistors. *IEEE Electron Device Lett.* 32, 2 (2011).
- Fortunato, E., Barquinha, P. & Martins, R. Oxide semiconductor thin-film transistors: A review of recent advances. *Adv. Mater.* 24, 2945, doi:10.1002/adma.v24.22 (2012).
- Lee, S. W., Suh, D., Lee, S. Y. & Lee, Y. H. Passivation effect on gate-bias stress instability of carbon nanotube thin film transistors. *Appl. Phys. Lett.* 104, 163506, doi:10.1063/1.4873316 (2014).
- Kim, S. I. *et al.* High performance oxide thin film transistors with double active layers. *IEDM Tech. Dig.* 73 (2008).
- Kim, T. S. *et al.* High performance gallium-zinc oxynitride thin film transistors for next-generation display applications. *IEDM Tech. Dig.* 660 (2013).
- Shih, C. W., Chin, A., Lub, C. F. & Yi, S. H. Extremely high mobility ultra-thin metal-oxide with ns<sup>2</sup>np<sup>2</sup> configuration. *IEDM Tech. Dig.* 145 (2015).
- Wu, Y. H., Yang, M. Y., Chin, A. & Chen, W. J. Electrical characteristics of high quality La<sub>2</sub>O<sub>3</sub> dielectric with equivalent oxide thickness of 5 Å. *IEEE Electron Device Lett.* 21, 341, doi:10.1109/55.847374 (2000).
- Wang, X. P. *et al.* Dual metal gates with band-edge work functions on novel HfLaO high- $\kappa$  gate dielectric. *Symp. on VLSI Tech. Dig.* 9 (2006).
- Cheng, C. F. *et al.* Very low V<sub>i</sub> [Ir–Hf]/HfLaO CMOS using novel self-aligned low temperature shallow junctions. *IEDM Tech. Dig.* 333 (2007).
- Wang, X. P. *et al.* Wide V<sub>th</sub> and V<sub>th</sub> tunability for metal gated MOS devices with HfLaO gate dielectrics. *IEEE Electron Device Lett.* 28, 258, doi:10.1109/LED.2007.891757 (2007).
- Lin, S. H., Liu, S. L., Yeh, F. S. & Chin, A. Low V<sub>i</sub> TaN/HfLaO n-MOSFETs using low temperature formed source-drain junctions. *IEEE Electron Device Lett.* 30, 75, doi:10.1109/LED.2008.2009011 (2009).
- Liao, C. C. *et al.* Metal-gate/high- $\kappa$ /Ge nMOS at small CET with higher mobility than SiO<sub>2</sub>/Si at wide range carrier densities. *IEEE Electron Device Lett.* 34, 163, doi:10.1109/LED.2012.2230241 (2013).

31. Lin, S. H. *et al.* High density and low leakage current MIM capacitor using stacked TiO<sub>2</sub>/ZrO<sub>2</sub> insulators. *IEEE Electron Device Lett.* **30**, 715, doi:[10.1109/LED.2009.2022775](https://doi.org/10.1109/LED.2009.2022775) (2009).
32. Chen, K. Y. *et al.* Influence of contact effect on the performance of microcrystalline silicon thin-film transistors. *Appl. Phys. Lett.* **89**, 203509, doi:[10.1063/1.2390634](https://doi.org/10.1063/1.2390634) (2006).
33. Chen, R. *et al.* Self-aligned top-gate InGaZnO thin film transistors using SiO<sub>2</sub>/Al<sub>2</sub>O<sub>3</sub> stack gate dielectric. *Thin Solid Films* **548**, 572, doi:[10.1016/j.tsf.2013.09.020](https://doi.org/10.1016/j.tsf.2013.09.020) (2013).
34. Im, S., Jin, B. J. & Yi, S. Ultraviolet emission and microstructural evolution in pulsed-laser-deposited ZnO films. *J. Appl. Phys.* **87**, 9 (2000).
35. Lin, S. S. & Huang, J. L. Effect of thickness on the structural and optical properties of ZnO films by r.f. magnetron sputtering. *Surf. Coat. Technol.* **185**, 222, doi:[10.1016/j.surfcoat.2003.11.014](https://doi.org/10.1016/j.surfcoat.2003.11.014) (2004).
36. Kim, W. K. *et al.* Stable high conductive amorphous InGaZnO driven by hydrogenation using hot isostatic pressing. *Appl. Phys. Lett.* **98**, 122109, doi:[10.1063/1.3567635](https://doi.org/10.1063/1.3567635) (2011).

## Acknowledgements

This paper's publication was supported in part by Ministry of Science and Technology of Taiwan.

## Author Contributions

C.W. Shih did the experiments; Albert Chin wrote the main manuscript text. All authors have given approval to the final version of the manuscript.

## Additional Information

**Supplementary information** accompanies this paper at doi:[10.1038/s41598-017-01231-3](https://doi.org/10.1038/s41598-017-01231-3)

**Competing Interests:** The authors declare that they have no competing interests.

The results of this research have important financial interests for both Display, ultra-low power 3D IC and CTFT.

**Publisher's note:** Springer Nature remains neutral with regard to jurisdictional claims in published maps and institutional affiliations.



**Open Access** This article is licensed under a Creative Commons Attribution 4.0 International License, which permits use, sharing, adaptation, distribution and reproduction in any medium or format, as long as you give appropriate credit to the original author(s) and the source, provide a link to the Creative Commons license, and indicate if changes were made. The images or other third party material in this article are included in the article's Creative Commons license, unless indicated otherwise in a credit line to the material. If material is not included in the article's Creative Commons license and your intended use is not permitted by statutory regulation or exceeds the permitted use, you will need to obtain permission directly from the copyright holder. To view a copy of this license, visit <http://creativecommons.org/licenses/by/4.0/>.

© The Author(s) 2017